Commun Nonlinear Sci Numer Simulat 152 (2026) 109362

Contents lists available at ScienceDirect

Communications in Nonlinear Science and Numerical Simulation

journal homepage: www.elsevier.com/locate/cnsns

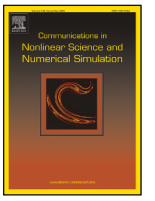

Research paper

Driving biofilms to finite time extinction by antibiotic cocktails

B. Birnir [a], A. Carpio [b,*], G. Duro [c]

[a] Universidad de California, Santa Bárbara, USA
[b] Universidad Complutense de Madrid, Spain
[c] Universidad Autónoma de Madrid, Spain

ARTICLE INFO

Keywords:
Finite time extinction
Nonlinear control
Transport-reaction-diffusion coupled systems
Antiobiotic treatment

ABSTRACT

Hospital acquired infections are often caused by biofilms growing on medical devices and implants. Biofilms are bacterial aggregates attached to wet surfaces that are glued together by a self-produced polymeric matrix. Devising protocols and therapies able to eradicate biofilms in medical environments is essential to prevent chronic infections, implant removal and sepsis. We present a simple model of combined antibiotic action which leads to extinction of a biofilm system in finite time. Slow death rates growing like powers ϕ^γ, $0 < \gamma < 1$, are key to achieve extinction. The model combines a nonlocal nonlinear transport equation with a quasi-stationary reaction-diffusion system, all set in a domain whose boundary moves with time. Estimates of extinction times suggest therapies based on administering large enough doses for a long enough time, or periodically for shorter times, validated by numerical simulations and theoretical results. Furthermore, we devise bang-bang and optimal control strategies based on Bucy-Kalman filters to achieve biofilm extinction in a given time through adequate antibiotic dosage. Interestingly, lower dosages with and abrupt final increase seem to suffice.

1. Introduction

Biofilms are the dominant habitat of bacteria in Nature. Bacteria adhere to moist surfaces and secrete a polymeric (EPS) matrix that envelops the bacterial community, acting as a shield against external aggressions [12]. As a result, the efficiency of disinfectants and antibiotics to eradicate biofilms is largely reduced [1,15].

Hospital acquired infections are often caused by biofilms [31]. They form on prostheses and medical equipment, leading to chronic infections, implant removal and septicaemia [33]. Antibiotics kill bacteria by targeting different processes. Popular antibiotics such as β-lactams (penicillins), glycopeptides (vancomycin), aminoglycosides (streptomycin), quinolones (ciprofloxacin) and tetracyclines are effective against active cells, that is, those actively dividing [2]. However, biofilms display a stratified structure depending on access to oxygen and nutrients [11]. Active cells concentrate in layers with higher levels of oxygen and nutrients. They are effectively killed by antibiotics targeting cell-wall synthesis, protein synthesis, DNA replication or translation, as those mentioned above. Poorly oxygenated regions contain dormant cells [13,34] instead. Killing dormant cells requires antibiotics targeting other processes. Polymixins (colistin), for instance, disrupt charge distributions in the membrane. Experimental studies show that it is possible to fully eradicate biofilms by antibiotic cocktails [13]. Mathematical modeling and simulation may guide the design of adequate treatments.

* Corresponding author.
E-mail address: ana_carpio@mat.ucm.es (A. Carpio).

https://doi.org/10.1016/j.cnsns.2025.109362
Received 22 May 2025; Received in revised form 22 August 2025; Accepted 21 September 2025
Available online 24 September 2025

A simple continuous model to study survival in antibiotic treated biofilms was proposed in [30]. The bacterial population diminishes, but does not vanish in finite time. More detailed agent based model of biofilm growth couple a cellular automata representation of biofilm geometry with a dynamic energy budget (DEB) description of cell metabolism, including the effect of antibiotics and EPS matrix production [5]. Numerical simulations show the formation of outer necrotic layers under the action of antibiotics targeting active cells. Carpio and González-Albaladejo [9] consider a more realistic representation of bacterial shapes and geometrical arrangements of bacteria within a biofilm by resorting to an immersed boundary framework. Bacteria immersed in a fluid matrix grow, divide and die according to DEB dynamics coupled to convection-reaction-diffusion equations for the concentration of nutrients, oxygen, waste and toxicants. By combining two types of antibiotics one can drive small biofilms to extinction in numerical simulations. However, in these agent based models cell death is a stochastic process. Numerical simulations produced specific realizations in which all bacteria died. It is not clear how to guarantee complete biofilm extinction in a given time for standard biofilms in medical applications due to the complexity and cost of these models, as well as the stochastic representation of some cell processes.

To investigate extinction phenomena in more detail, here we work in a deterministic framework. We consider a modification of the continuous model proposed in [30] that combines two antibiotic types: one of them targets outer layers of active cells whereas the other one targets the core inner layer of dormant cells. We observe that death rates associated with the selected antibiotics must involve 'slow' power laws of the volume fractions to achieve finite time extinction. Otherwise, theoretical studies of the continuous model can only guarantee a decrease to zero of the volume fraction of alive bacteria as time grows. The relevance of slow absorption terms in achieving finite time extinction in a variety of applications has long been observed, see [3,4,19,21,26] and references therein, for instance. In our framework, we reach the extinction goal by either administering large enough concentrations of antibiotic cocktails during a long enough interval or by periodically delivering a cocktail until the population is completely depleted. Our estimates of the extinction time as a function of the model parameters can guide the design of dosages. For practical applications, we develop bang-bang and optimal control strategies to reach finite time extinction through antibiotics. While bang-bang methods administer large doses periodically, Bucy-Kalman filters supply a continuous inflow of smaller antibiotic concentrations.

The rest of the paper is organized as follows. Section 2 illustrates the extinction dynamics on a transport problem. We present the biofilm model in Section 3, together with simulations of biofilm eradication by antibiotic cocktails. Section 4 discusses a possible practical implementation, while Sections 5 and 6 devise simple bang-bang and optimal control strategies. Details about the procedure used for numerical simulations are given in Section 7. Some theoretical properties of the model supporting the extinction simulations and estimates are summarized in Section 8. Well posedness results are established. Finally, Section 9 discusses our conclusions and future perspectives.

2. Finite time extinction in linear transport problems

Finite time extinction in partial differential equations is usually a consequence of the presence of adequate absorption terms. Let us illustrate the idea on a simple linear transport problem

$$\begin{aligned} &\phi_t + a(x,t)\phi_x = -g(\phi),\ x \in \mathbb{R}, t > 0, \\ &\phi(x,0) = 0, \end{aligned} \tag{1}$$

for $a : \mathbb{R} \times \mathbb{R}^+$. Along the characteristic curves $x'(t) = a(x(t),t)$, $t \geq 0$, the partial differential equation becomes an integrable differential equation [24]

$$\frac{d\phi(x(t),t)}{dt} = -g(\phi(x(t),t)) \implies \int_{\phi(x(t),t)}^{\phi(x_0,0)} \frac{d\phi}{g(\phi)} = t.$$

Whenever $\int_0^{\phi(x_0,0)} \frac{d\phi}{g(\phi)} = t_{x_0} < \infty$, $\phi(x(t),t)$ vanishes at time t_{x_0}.

A typical absorption term is $g(\phi) = \phi^\gamma$, $0 < \gamma < 1$. Then $\int_0^{\phi_0} \phi^{-\gamma} d\phi = \frac{\phi_0^{-\gamma+1}}{-\gamma+1} = t_0$. The solution along characteristics is given by

$$\begin{aligned} &\frac{\phi(x(t),t)^{-\gamma+1}}{-\gamma+1} - \frac{\phi(x(0),0)^{-\gamma+1}}{-\gamma+1} = -t \implies \\ &\phi(x(t),t) = (-(1-\gamma)t + \phi(x(0),0)^{-\gamma+1})^{1/(1-\gamma)}. \end{aligned} \tag{2}$$

The values of ϕ along this characteristic curve vanish for $t \geq \frac{\phi(x(0),0)^{-\gamma+1}}{-\gamma+1}$. Notice that this time tends to infinity as $\gamma \to 1$. As illustrated by Fig. 1(a), the values of ϕ^γ for $0 < \gamma < 1$ are larger than the corresponding ones for $\gamma > 1$. This results in solutions decreasing faster. This phenomenon has been often observed in nonlinear diffusion equations with fractionary diffusion and absorption [3,4,19,21,26].

Expression (2) can be used to define the solution $\phi(x,t)$ of (1) everywhere when for any point (x,t) we can find a unique value x_0 such that the characteristic curve $x(t;x_0)$ with initial datum x_0 reaches x at time t. If a is constant, $x(t;x_0) = x_0 + at$. Thus, for any (x,t) lying on a characteristic curve, the corresponding x_0 is given by $x_0 = x - at$. As a result,

$$\phi(x,t) = (-(1-\gamma)t + \phi(x-at,0)^{-\gamma+1})^{1/(1-\gamma)}.$$

Fig. 2 plots this solution for specific choices of data and parameters to illustrate the spatio-temporal dynamics of the extinction process.

Simple models for biofilm growth in slabs, display a similar structure, as we will see next.

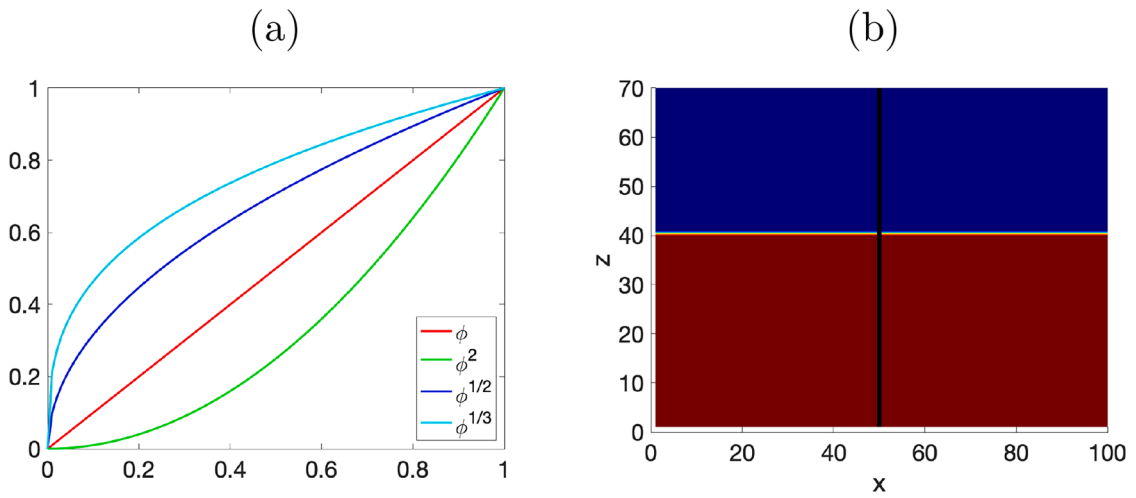

Fig. 1. (a) Power-like absorption sources $g(\phi) = \phi^{\gamma}$ for different values of γ. (b) Illustration of the biofilm geometry used in the simulations. We consider a vertical cut of a biofilm slab, represented by the black line. The biofilm occupies the bottom red area whereas the upper blue part represents an external medium bringing oxygen, nutrients and/or toxicants.

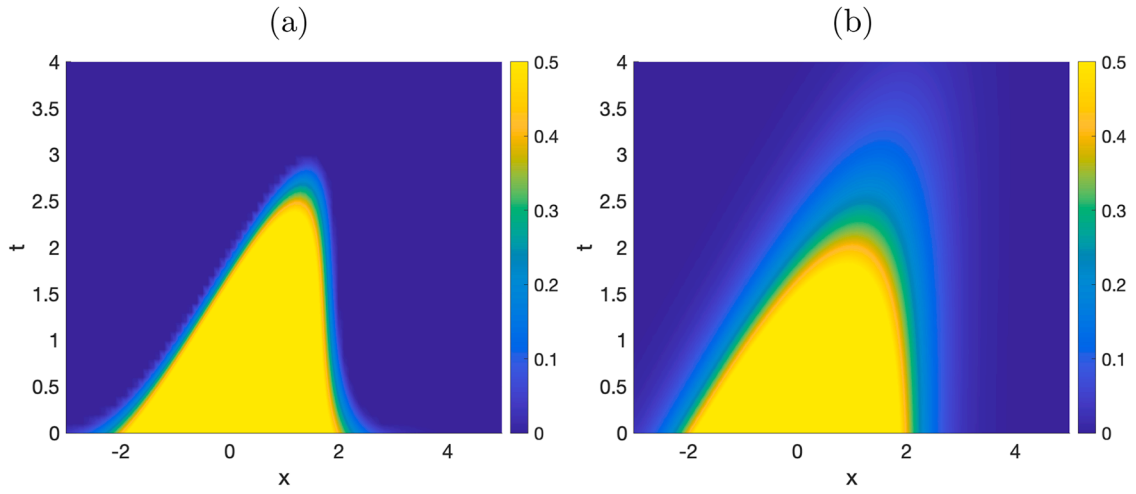

Fig. 2. Top view of the solutions $\phi(x,t)$ of (1) for (a) $\gamma = 0.1$, (b) $\gamma = 0.9$ with $\phi(x,0) = 3\exp(-0.5x^2)$ and $a = 0.5$. Notice that as γ gets closer to 1 the time for complete extinction increases.

3. Extinction in balance laws for biofilms under the effect of antibiotics

The slab geometry in Fig. 1(b) allows us to gain insight on the extinction process by means of basic conservation law models. We consider here a one dimensional approximation.

3.1. Model equations

Let ϕ_{d} and ϕ_{l} denote the volume fractions of dead and alive cells in the biofilm, respectively. The concentrations of oxygen and antibiotics are C_{o}, C_{a_1} and C_{a_2}, respectively. Cell volume fractions are subject to the constraints

$$\phi_{\mathrm{d}} + \phi_{\mathrm{l}} = 1, \quad 0 \le \phi_{\mathrm{d}}, \phi_{\mathrm{l}} \le 1. \tag{3}$$

We modify the balance law for live cells proposed in [30], including two sinks representing two types of antibiotics instead of one, to get

$$\frac{\partial \phi_{\mathrm{l}}}{\partial t} = \mu(e)\phi_{\mathrm{l}} - \frac{\partial (v\phi_{\mathrm{l}})}{\partial z} - k_{\mathrm{a}_1}(e)C_{\mathrm{a}_1}\phi_{\mathrm{l}}^{\gamma_1} - k_{\mathrm{a}_2}(e)C_{\mathrm{a}_2}\phi_{\mathrm{l}}^{\gamma_2}, \tag{4}$$

for $0 < z < L(t)$, $t > 0$, with initial conditions

$$\phi_{\mathrm{l}}(z,0) = 1, \quad 0 \le z \le L(0), \tag{5}$$

where $L(0)$ is the height $L(t)$ of the slab at time $t = 0$. The advective velocity satisfies

$$\frac{\partial v}{\partial z} = \mu\phi_1,\ 0 < z < L(t), \quad v(0,t) = 0,\ t > 0. \tag{6}$$

The biofilm thickness $L(t)$ is given by [30]

$$\frac{\partial L(t)}{\partial t} = v(L(t),t) - k_d L(t)^2, \quad t > 0, \tag{7}$$

k_d being the detachment rate coefficient. The growth and death rates depend on the liming concentration for biofilm growth, that is, the concentration of oxygen C_o, through the local energy $e = \frac{C_o}{C_o+K_o}$. We define absorption coefficients for the antibiotics depending on the energy level, so that one targets the cells with hight energy levels, while the other one targets dormant layers with little energy:

$$\mu(e) = \mu_{\max} e,\ k_{a_1}(e) = k_1\eta(e)e,\ k_{a_2}(e) = k_2(1-\eta(e))(e_{\max} - e), \tag{8}$$

where K_o stands for the oxygen Monod half-saturation coefficient and $e_{\max} = \frac{c_{o,\max}}{c_{o,\max}+K_o}$. Here, μ represents the specific growth rate at any point [30], whereas k_{a_1} and k_{a_2} stand for the death rates for antibiotics targeting active cells (large energy) and dormant cells (low energy), respectively [5,9]. The smooth function $\eta(e)$ increases sharply from zero to one. In this way one antibiotic is active for small values of e and the other one for larger values.

In the computational region $0 \le z \le L_{\max}$, with $L(t) \ll L_{\max}$, $t > 0$, the concentrations of oxygen and antibiotic obey

$$\begin{aligned}
&\frac{\partial C_o}{\partial t} = \frac{\partial}{\partial z}\left(d_o \frac{\partial C_o}{\partial z}\right) - k_o \frac{C_o}{C_o + K_o}\phi_1\chi_{[0,L(t)]}\phi_c\rho_x, && 0 < z < L_{\max}, t > 0,\\
&C_o(z,0) = c_o', && 0 \le z \le L_{\max},\\
&\frac{\partial C_o}{\partial z}(0,t) = 0, && t > 0,\\
&C_o(L_{\max},t) = c_o, && t > 0,
\end{aligned} \tag{9}$$

$$\begin{aligned}
&\frac{\partial C_a}{\partial t} = \frac{\partial}{\partial z}\left(d_a \frac{\partial C_a}{\partial z}\right) - k_a C_a\phi_1\chi_{[0,L(t)]}\phi_c\rho_x, && 0 < z < L_{\max}, t > 0,\\
&C_a(z,0) = c_a', && 0 \le z \le L_{\max},\\
&\frac{\partial C_a}{\partial z}(0,t) = 0, && t > 0,\\
&C_a(L_{\max},t) = c_a, && t > 0,
\end{aligned} \tag{10}$$

for the two types of antibiotics $a = a_1, a_2$. Here, d_o and d_a represent the diffusion coefficients for oxygen and antibiotics inside and outside the biofilm, k_o and k_a the oxygen and antibiotic reaction rates, ρ_x the bacterial density and ϕ_c the cell fraction of the total biofilm volume. $\chi_A(z)$ represents the characteristic function of set A, that is, 1 in A and zero otherwise.

This model is a modification of the model proposed in [30], that includes two antibiotics and reformulates the concentration equations as a transmission problem for simplicity. Moreover, we allow for 'slow' death rates with $0 < \gamma_1, \gamma_2 < 1$, while [30] sets $\gamma_1 = \gamma_2 = 1$. Values for the model parameters are given in [30] for *Pseudomonas Aureginosa* and [5,9] for different antibiotic types.

Notice that the transport Eq. (4) is set in a domain $\Omega^t = \{z \,|\, 0 < z < L(t)\}$ whose boundary moves with time. Transport equations only require boundary conditions on the boundary $\partial\Omega^t$ when the scalar product of the outer normal vector and the velocity at the boundary points is negative [23]. Since $v(0,t) = 0$, $t > 0$, no boundary condition on $\phi_1(z,t)$ is required at $z = 0$. Since $v(L(t),t)$ is expected to be nonnegative, no boundary condition is required at $z = L(t)$ either. Thus, the fact the model is set on a moving domain is not an obstacle to formulate numerical schemes for the transport problem as long as the concentration fields are known, see Section 7.1. Establishing theoretical well posedness results, however, is a challenge. We have been able to do so assuming that the boundary retracts in Section 8.2. Dealing with time dependent reaction-diffusion problems such as (9) and (10) set in moving domains Ω^t is also a demanding issue, see [7] for a discussion and for some general results for specific types of moving boundaries. Here, we will make use of the time scale separation in the transport and diffusion submodels to resort to a quasi-stationary approximation, replacing (9) and (10) by elliptic problems, see Sections 7.2 and 8.1. The next section illustrates some extinction results obtained in this regime.

3.2. Extinction simulations

Fig. 3 illustrates the extinction process starting from a uniform initial volume fraction $\phi_1(z,0) = 1$, $0 \le z \le 5$, $\phi_1(z,0) = 0$, $5 < z \le 10$, in a computational slab of length $L_{\max} = 10$. Panel (a) represents the initial 'energy' e and antibiotic concentration. Panel (b) visualizes extinction in finite time of ϕ_1, while (c) depicts the local 'energy' e and the antibiotic concentration at the final time. For simplicity, we have taken the same antibiotic parameters for both antibiotics, but different death rates as described in (8). We have selected $\eta(e) = (1 + \tanh(100(e - 0.05)))/2$ and $\gamma_1 = \gamma_2 = 1/2$. Other parameter values for the simulations are collected in Table 1. When we switch to $\gamma_1 = \gamma_2 = 1$, the volume fraction $\phi_1(z,t)$ decreases to zero without becoming zero, as shown in panel (d).

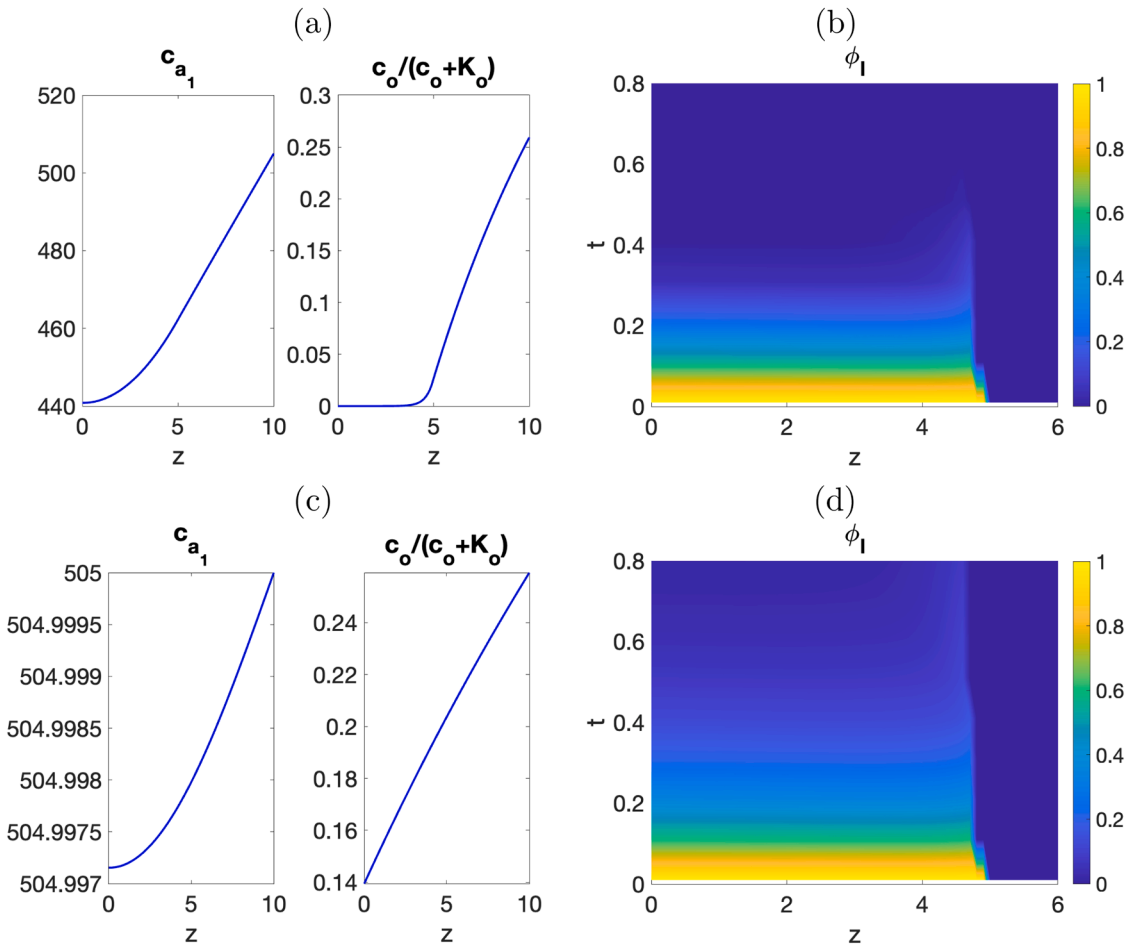

Fig. 3. Extinction process for a cocktail of two antibiotics with death rates given by (8): (a) Initial antibiotic and energy profiles. For $\gamma_1 = \gamma_2 = 0.5$ (b) time evolution of ϕ_1 and (c) antibiotic and energy profiles at the end of the computation. By time 0.58 h, ϕ_1 vanishes everywhere. (d) Time evolution of ϕ_1 for $\gamma_1 = \gamma_2 = 1$. As time grows, it decreases to zero, but it remains positive.

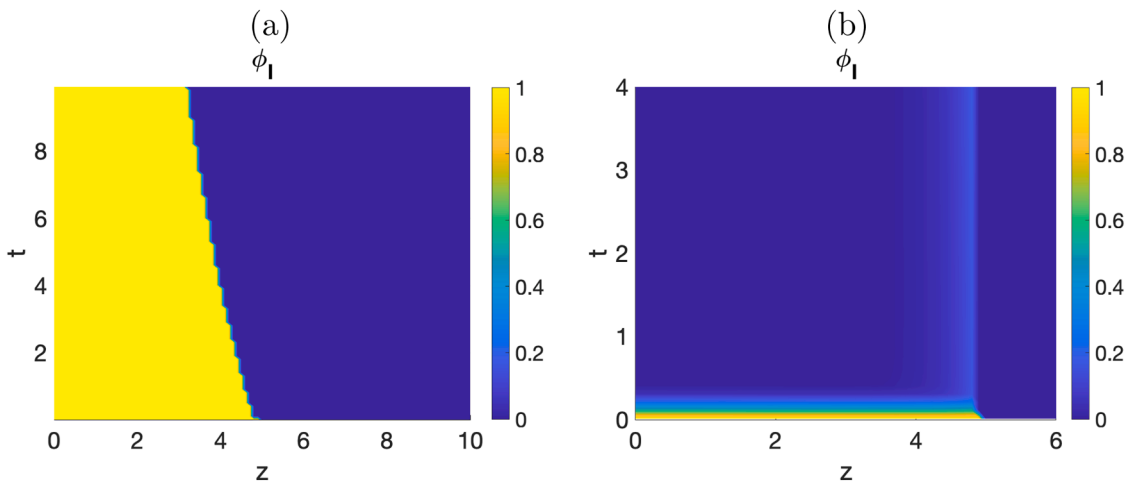

Fig. 4. (a) Treatment with an antibiotic only targeting active cells dividing fast. (b) Treatment with an antibiotic targeting only dormant cells with low activity.

Table 1
Parameter values for the simulations.

c_o	c_a	d_o	d_a
0.035 [mg/l]	505 [mg/l]	2.2 · 1e4 [$\mu m^2/s$]	0.5 · 1e4 [$\mu m^2/s$]
k_o	k_a	K_o	ρ_x
0.30/0.24 [1/h]	0.0016 [l/(mg h)]	0.1 [mg/l]	47,000 [mg/l]
ϕ_c	μ_{max}	k_1	k_2
0.1	0.3 [1/h]	0.0385 [l/(mg h)]	0.0385 [l/(mg h)]

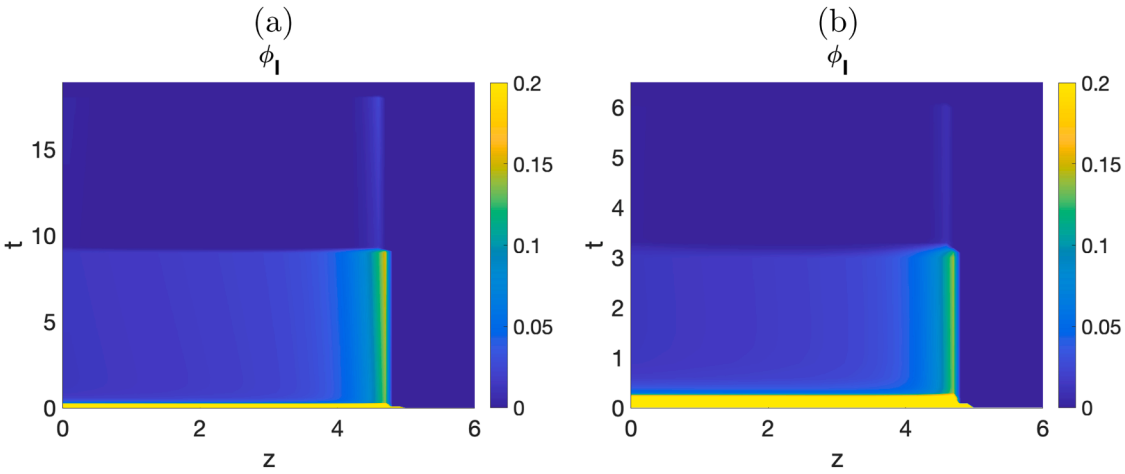

Fig. 5. Antibiotic cocktail applied periodically during 0.3 h: (a) at intervals of 9 h, alive bacteria extinguish after 18.2 h, (b) at intervals of 3 h, alive bacteria extinguish after 6.1 h. Other parameters as in Fig. 3(b)–(c).

Instead, Fig. 4 illustrates the behavior of the system when we use a single antibiotic type. Either the outer layer or the inner part remains alive. The relative appearance depends on the concentrations used. In panel (a), the outer layer of dead cells detaches gradually.

In these simulations, we discretize the transport model by an upwind-scheme and the additional differential constraint by progressive finite differences. Notice that we do not need boundary conditions for ϕ_l at $z = 0$ because $v(0, t) = 0$. Provided ϕ_l remains positive in time, the velocity v is positive too. The characteristic curves of the transport problem [24] enter the boundary $z = L(t)$, so that no boundary condition is required at that wall either. The reaction-diffusion submodels evolve in a much faster scale and relax to quasi-stationary states in seconds. We can employ finite elements if the diffusion coefficients are discontinuous at $L(t)$, otherwise a time relaxation scheme with finite differences in space works. It is essential that the selected scheme preserves positivity for stability, together with the constraint $\phi_l \leq 1$, as will discuss in Section 7.

4. Designing therapies to eradicate biofilms

The previous section suggests that we may be able to eradicate biofilms by administering large enough concentrations of antibiotic cocktails during a long enough time interval. A continuous infusion of low dosages may keep the infection in a chronic state, instead. A periodic sequence of as large doses as possible for as long time intervals as tolerable can reduce the volume fractions of alive bacteria in successive steps until the time interval and the doses selected are enough to kill all remaining bacteria, see Fig. 5.

In practical applications, it is difficult to calibrate the magnitude of the doses for finite time extinction. Moreover, toxicity effects on a patient may impose additional size constraints. The following upper and lower estimates of extinction times as a function of concentrations and volume fractions may suggest educated choices.

Eqs. (4) and (6) yield

$$\frac{\partial \phi_l}{\partial t} + v\frac{\partial \phi_l}{\partial z} = \mu(e)(\phi_l - \phi_l^2) - k_{a_1}(e)C_{a_1}\phi_l^{\gamma_1} - k_{a_2}(e)C_{a_2}\phi_l^{\gamma_2},$$

with $0 < \gamma_1, \gamma_2 < 1$. Assume that, as expected, $0 \leq \phi_l \leq 1$. Then, $v(z,t) = \int_0^z \mu(e(s,t))\phi_l(s,t)ds \geq 0$ and $v(z,t) \leq L(t)\mu_{max}$.

For $v = 0$ and freezing the coefficients at $t = 0$, we have

$$\frac{\partial \phi_l}{\partial t} = \mu(e(0))\phi_l(1 - \phi_l) - k_{a_1}(e(0))C_{a_1}(0)\phi_l^{\gamma_1} - k_{a_2}(e(0))C_{a_2}(0)\phi_l^{\gamma_2},$$

for each $0 < z < L(0)$. Set

$$f(z,\phi_1) = -\mu(e(z,0))\phi_1(1-\phi_1) + k_{a_1}(e(z,0))C_{a_1}(z,0)\phi_1^{\gamma_1} + k_{a_2}(e(z,0))C_{a_2}(z,0)\phi_1^{\gamma_2}.$$

Then, lower bounds of the extinction times t^- for each z are given by

$$t^-(z) = \int_0^{\phi_1(z,0)} \frac{d\phi_1}{f(z,\phi_1)} \geq \int_0^1 \frac{d\phi_1}{(k_{a_1}(e(z,0))C_{a_1}(z,0) + k_{a_2}(e(z,0))C_{a_2}(z,0))\phi_1^{\min(\gamma_1,\gamma_2)}}$$
$$= \frac{1}{k_{a_1}(e(z,0))C_{a_1}(z,0) + k_{a_2}(e(z,0))C_{a_2}(z,0)} \frac{1^{-\min(\gamma_1,\gamma_2)+1}}{(-\min(\gamma_1,\gamma_2)+1)}.$$

Varying z over $[0, L(0)]$, the minimum value provides a lower estimate of the extinction time.

For $\nu = \nu_{\max}$, following Section 2, we get the following upper bounds

$$t^+(z) = \int_0^{\phi_1(z_0,0)} \frac{d\phi_1}{f(z,\phi_1)} = \int_0^1 \frac{d\phi_1}{f(z,\phi_1)}$$

for $z^0 = z - \nu t$ and $\phi_1(z,0) = 1$. Varying z over $[0, L(0)]$, the maximum value provides an upper estimate of the extinction time.

5. Bang-Bang control to achieve biofilm extinction in a given time

For practical applications, it is important to know what antibiotic concentrations we need to eradicate a biofilm in a given time. We can devise a procedure to do so employing model (3)–(10) by first analyzing simpler models.

The control of nonlinear systems often relies on controlling first linearized versions about equilibrium states of the uncontrolled problem. Bang-bang approaches typically implement feedback controllers that switch between two states [29]. The uncontrolled transport problem we address here has two equilibrium states: 0 and 1. To drive the system from 1 to 0 we introduce a strategy that first linearizes about 1 and drives the system to a state b closer to 0 by choosing an antibiotic concentration value. Next, we linearize about zero and drive the system from b to zero choosing a different antibiotic concentration value. We illustrate the idea next on a model differential equation and then extend it to the transport problem under study.

5.1. Control of key ordinary differential equations

For $0 < \gamma < 1$, we consider the problem

$$\phi' = \mu(\phi - \phi^2) - kc\phi^\gamma, \quad \phi(0) = 1, \tag{11}$$

where c is the control that drives $\phi(0) = 1$ to $\phi(T) = 0$, $T > 0$. The uncontrolled part, $v' = \mu(v - v^2)$, has constant solutions $v = 0$ and $v = 1$. Making the change $\phi = 1 + \hat{\phi}$, (11) becomes

$$\hat{\phi}' = \mu(-\hat{\phi} - \hat{\phi}^2) - kc(1+\hat{\phi})^\gamma, \quad \hat{\phi}(0) = 0,$$

where c is the control that drives $\hat{\phi}(0) = 0$ to $\hat{\phi}(T) = -1$. When $\hat{\phi}$ is small, $\hat{\phi} \sim 0$, we can linearize about 0 neglecting the low order term $\hat{\phi}^2$ and using $(1+\hat{\phi})^\gamma \sim 1 + \gamma(1+0)^{\gamma-1}\hat{\phi}$ to get

$$w' = -\mu w - kc - kc\gamma w = -(\mu + kc\gamma)w - kc, \quad w(0) = 0,$$

whose solution is

$$w(t) = \frac{-kc}{\mu + kc\gamma}\left(1 - e^{-(\mu+kc\gamma)t}\right). \tag{12}$$

Let us estimate c to achieve $w(T) = -a$. We need

$$1 - \frac{a(\mu + kc\gamma)}{kc} = e^{-(\mu+kc\gamma)T} \implies \tag{13}$$

$$-(\mu + kc\gamma)T = \ln\left(1 - \frac{a(\mu+kc\gamma)}{kc}\right). \tag{14}$$

Taylor expanding the logarithm, we get $-\frac{a(\mu+kc\gamma)}{kc} = -(\mu + kc\gamma)T$ to first order, which yields an estimate $c \sim \frac{a}{kT}$. Depending on the parameter values, an alternative estimate follows by calculating c such that $\frac{kc}{\mu+kc\gamma} = a$. We use these estimates to generate starting values for a Newton scheme to find an accurate solution of the nonlinear Eq. (14). The full Eq. (11) including the term $-\phi^2$ will reach a value lower than $b = 1 - a$. We can choose, for instance, $a = 0.5$.

Next, we go from b to 0. Consider

$$\phi' = \mu(\phi - \phi^2) - kc\phi^\gamma, \quad \phi(0) = b,$$

where c is the control that drives $\phi(0) = b$ to $\phi(T) = 0$. For $\hat{\phi} \sim 0$ small, we can neglect low order terms ϕ^2 and work with $v' = \mu v - kcv^\gamma$, $v(0) = b$. Making the change of variables $w = e^{-\mu t}v$, $w' = -\mu e^{-\mu t}v + e^{-\mu t}v'$, we find

$$w' = -kce^{\mu(\gamma-1)t}w^\gamma, \quad w(0) = b.$$

Separating variables, we obtain the solution

$$\frac{w^{-\gamma+1}(t) - b^{-\gamma+1}}{-\gamma+1} = -\frac{1}{\mu(\gamma-1)} kc(e^{\mu(\gamma-1)t} - 1)$$

that is,

$$w(t) = \left(b^{-\gamma+1} + \frac{1}{\mu} kc(e^{\mu(\gamma-1)t} - 1) \right)^{\frac{1}{1-\gamma}}.$$

This solution vanishes at time T if

$$c = \frac{\mu}{k(1 - e^{\mu(\gamma-1)T})} b^{-\gamma+1}. \tag{15}$$

Notice that $1 - e^{\mu(\gamma-1)T} > 0$ since $0 < \gamma < 1$. This suggests a procedure to drive the solution of (11) to zero. The previous equations are controlled in an exact way. When adding the discarded nonlinear terms, we can expect small errors. First, we set c in (11) equal to the solution of (14) with $a = 0.5$ and reach a value smaller than 0.5 at time T. Then, we set c in (11) equal to (15) and reach a value close to zero at time $2T$. Numerical simulations show that solving for a time $2T$, or slightly larger, we reach zero. T has no significance here, beyond being the time it takes to reduce the solution by a factor of 1/2. It is then natural to check if the solution is reduced to zero in twice that time, or in time $2T$. In the next sections, we extend this idea first to the transport problem and finally to the biofilm model, for which we illustrate the results numerically.

5.2. Control of the conservation law

Les us consider the conservation law for the fraction of live cells

$$\frac{\partial \phi}{\partial t} + v \frac{\partial \phi}{\partial z} = \mu(\phi - \phi^2) - kc\phi^\gamma, \tag{16}$$

where $v(z,t) = \int_0^z \mu\phi \, ds$. We seek c driving ϕ to zero everywhere in a given time. The uncontrolled part

$$\frac{\partial \phi}{\partial t} + v \frac{\partial \phi}{\partial z} = \mu(e)(\phi - \phi^2)$$

has constant solutions 1 and 0. As in Section 5.1, the idea is to linearize first about 1 to drive the system to smaller values near 0.5 and then about 0 to drive the system from 0.5 to zero.

Making the change $\phi = \hat{\phi} + 1$, we get

$$\frac{\partial \hat{\phi}}{\partial t} + \hat{v} \frac{\partial \hat{\phi}}{\partial z} = \mu(-\hat{\phi} - \hat{\phi}^2) - kc(1 + \hat{\phi})^\gamma, \quad \hat{\phi}(0) = 0,$$

where $\hat{v}(z,t) = \int_0^z \mu(1 + \hat{\phi}) ds$ and c is the control that drives $\hat{\phi}(0) = 0$ to $\hat{\phi}(T) = -1$. Linearizing about 0, we get

$$\frac{\partial w}{\partial t} + \mu z \frac{\partial w}{\partial z} = -\mu w - kc - k\gamma c w = -(\mu + k\gamma c)w - kc, \quad w(0) = 0.$$

The characteristic curves for this equation [24] are solutions of

$$z'(t) = \mu z(t) \implies z(t) = z_0 e^{\mu t}, \; t \geq 0.$$

Along the characteristic curves, $w(t) = w(z(t), t)$ satisfies

$$w'(t) = -(\mu + k\gamma c)w - kc, \quad w(0) = w(z_0, 0) = 0.$$

We have studied this ordinary differential equation in Section 5.1. If we choose c according to (14), we can drive the whole system to a value b, for instance, 0.5, at a time T. Notice that we can reconstruct the solution of the conservation law $w(z,t)$ using the characteristic curves. Given any point (z,t) in the computational region considered, we can find a unique curve $z(t; z_0)$ corresponding to an initial value z_0 such that $z(t; z_0) = z$. In fact, $z_0 = ze^{-\mu t}$ and $w(z,t) = w(z(t; z_0), t) = w(t)$ given by (12) always, since z_0 does not change the curve.

Next, we neglect low order terms when $\phi \sim 0$ in (16) to get

$$\frac{\partial w}{\partial t} = \mu w - kcw^\gamma, \quad w(0) = b.$$

We have also studied this equation in Section 5.1. If we choose c according to (15), we can drive the system near 0, at a time T.

Combining both steps, we devise a procedure to drive the solution of (16) to zero. The previous approximate equations are controlled in an exact way. When adding the nonlinear terms we have discarded, we expect small errors. First, we set c in (16) equal to the solution of (14) with $a = 0.5$ and reach a value slightly smaller than 0.5 at time T. Then, we set c in (16) equal to (15) and reach a value close to zero at time $2T$. Numerical simulations show that solving for a slightly larger time than $2T$ we reach zero.

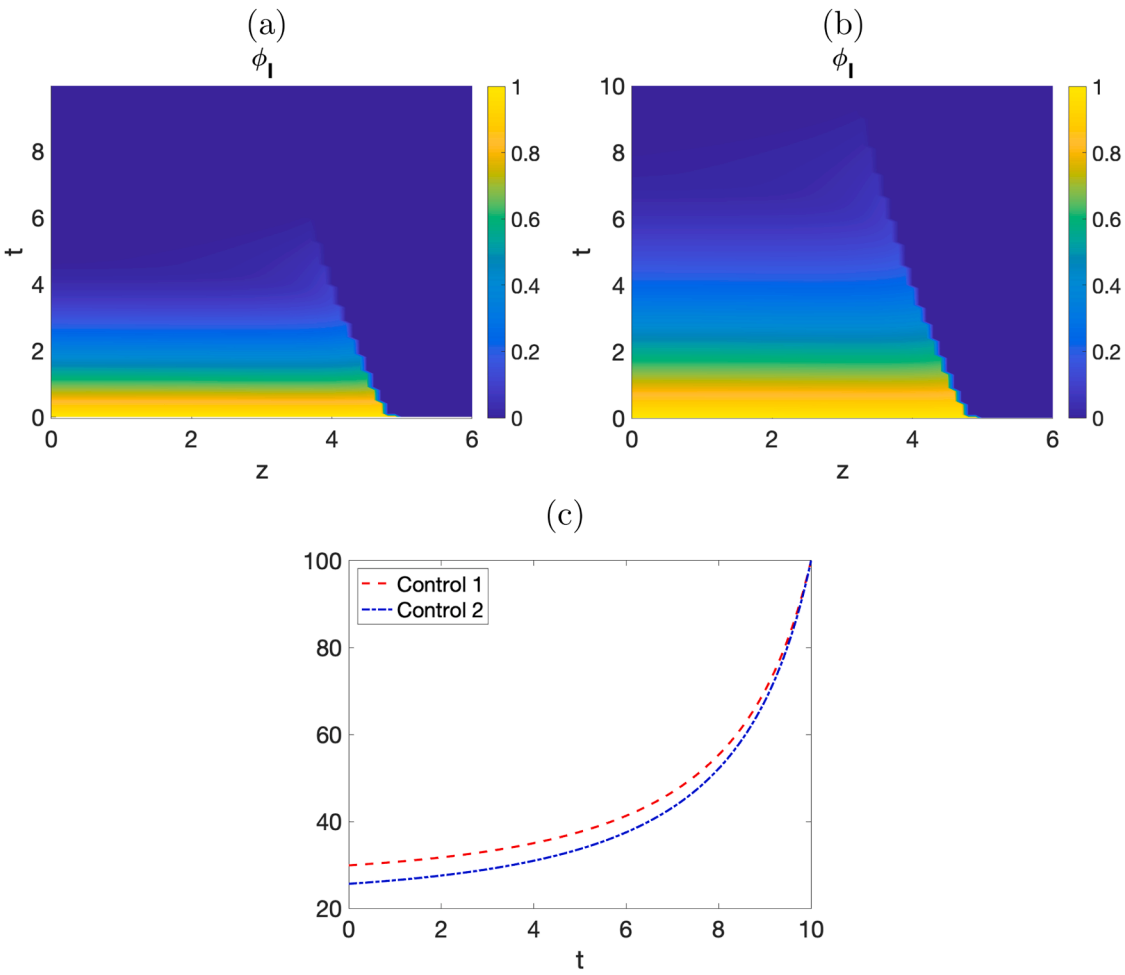

Fig. 6. Antibiotic cocktail infused during 10 h. (a) Following the Bang-Bang control procedure. We infuse constant concentrations $c_{a_1} = 38.9$ and $c_{a_2} = 38.86$ half of the time and 95.5 for the remaining half. (b) Following the optimal control procedure with $\epsilon = 10^{-4}$. The concentration profiles infused are depicted in panel (c) for c_{a_1} (dashed) and c_{a_2} (dotted-dashed).

5.3. *Control of the biofilm model*

The equations governing the biofilm (3)–(10), involve a conservation law of the form (4). Now the coefficients μ and k are not constant, but depend on $e = c_o/(c_o + K_o)$. We see in Fig. 3(a) that $e(z)$ decreases as we move deep into the biofilm. To estimate the concentrations, we use the reference values for the middle depth $z = 5$: $\mu = \mu(e(5))$ and $k = k_{a_1}(e(5))$ in the formulas derived in Sections 5.1 and 5.2.

We have implemented the following control strategy:

- In a first step, we choose the concentration c given by (14) with $\mu = \mu(e(5))$ and $k = k_{a_1}(e(5))$ and solve (3)–(10) with the parameters for Fig. 3(b)–(c) for a given a time T and $a = 0.5$, setting $C_{a_1} = C_{a_2} = c$ and starting from $\phi_l(0) = 1$ everywhere. Numerically, we observe that $\phi_l(z, T)$ becomes smaller that 0.5 everywhere.
- In a second step, we choose the concentration given by (15) with $\mu = \mu(e(5))$ and $k = k_{a_1}(e(5))$ and solve (3)–(10) with the parameters for Fig. 3(b)–(c) for a given a time T, setting $C_{a_1} = C_{a_2} = c$ and starting from the previous state $\phi_l(z, T)$ everywhere.

The second step usually employs higher antibiotic concentrations. Numerically, we observe that $\phi_l(z, 2T)$ is zero thanks to the fractionary values of γ_1 and γ_2, see Fig. 6(a).

6. Optimal control to achieve biofilm extinction in a given time

The Bang-Bang control we have implemented in the previous section may force the use of high doses, which may not be acceptable when applied to a human (biofilms in implants or prostheses). In this section, we propose an optimal control strategy based on

continuous infusion of controlled dosages, more specifically, by means of Kalman filters. We will first recall some background on optimal control theory and then particularize it for the biofilm control problem.

6.1. Optimal control essentials

Let us consider the linear regulator problem solved by Kalman [16,17]. We start with a linear partial differential equation for the output $x(t)$,

$$\dot{x} = Ax + Bu, \quad x(0) = x_0, \tag{17}$$

where x lies in a Banach space X and we seek the control minimizes the cost function

$$J(x) = \frac{1}{2}\langle x(t_f), Px(t_f)\rangle + \frac{1}{2}\int_{t_0}^{t_f} \langle x(t), Sx(t)\rangle dt + \langle u, Ru\rangle$$

with a given final time t_f. A, P and S are operators on X satisfying various technical conditions that are specified below. The input u lies in Banach space U, where the operator B acts. R is a bounded operator on U also satisfying some technical conditions, see [10]. $\langle\,\rangle$ denotes the dual parings between X, U and their dual spaces $X^\dagger$, $U^\dagger$.

If we take Eq. (17) as a constraint and look for the maximum of the Hamiltonian

$$H(x) = \frac{1}{2}\langle x(t), Sx(t)\rangle + \frac{1}{2}\langle u, Ru\rangle + \langle \lambda, Ax\rangle + \langle \lambda, Bu\rangle$$

$\lambda \in X^\dagger$ being the Lagrange multiplier that satisfies the terminal condition,

$$\lambda(t_f) = Px(t_f),$$

then a necessary condition for H (and J) to have a maximum is that the functional variations of H satisfy

$$\frac{\delta H}{\delta u} = Ru + B^*\lambda = 0$$

and

$$-\dot{\lambda} = \frac{\delta H}{\delta x} = Sx + A^*\lambda, \tag{18}$$

stars denoting the adjoint operators. The former equation above has the solution

$$u(t) = -R^{-1}B^*\lambda(t). \tag{19}$$

If we seek a solution of Eq. (18) of the form $\lambda = Qx$, we get

$$\dot{Q}x + Q\dot{x} = -Sx - A^*Qx. \tag{20}$$

Using (17) and (19)–(20), we find

$$\dot{Q}x + QAx - QBR^{-1}B^*Qx = -Sx - A^*Qx. \tag{21}$$

We conclude that Q must satisfy the Ricatti equation [14,16]

$$\dot{Q}(t) = -Q(t)A - A^*Q(t) + Q(t)BR^{-1}B^*Q(t) - S, \qquad Q(t_f) = P, \tag{22}$$

since (21) holds for general x in X. The Ricatti Eq. (22) is solved backward to obtain the operator

$$K(t) = -R^{-1}B^*Q(t)$$

called the *Kalman gain*, and the *closed-loop optimal feedback control* is computed by applying K to the solution,

$$u(t) = K(t)x(t).$$

This procedure is called a *linear regulator* and it is a linear feedback control law. If we compute the second variation of J, we see that the operators P, S and R must be at least non-negative definite. The precise conditions are given in [10].

The maximum principle that we have used is called the Pontryagin maximum principle, see [28]. An equivalent method finds the cost function $J = V$ by solving the Hamilton-Jacobi (Bellmann) equation

$$\dot{V}(x,t) = -H(x, \frac{\partial V}{\partial x}, t), \tag{23}$$

with the initial condition $V(x(t_f), t_f) = \frac{1}{2}\langle x(t_f), Px(t_f)\rangle$, see [25].

6.2. Control of the model equation

As we did with Bang-Bang control, we can think of first driving the solution to $\phi = 1/2$ by linearizing about $\phi = 1$ and then, linearize about a small value $\phi = \epsilon$ to reach zero. We use optimal control in these two steps to drive the solution to zero.

Linearizing the problem

$$\frac{\partial \phi}{\partial t} + v\frac{\partial \phi}{\partial z} = \mu(\phi - \phi^2) - kc\phi^\gamma, \quad \phi(0) = 1, \quad v = \int_0^z \mu\phi ds,$$

about ϕ, we find

$$\frac{\partial w}{\partial t} + v\frac{\partial w}{\partial z} = \mu(1-2\phi)w - \frac{\gamma kc}{\phi^{1-\gamma}}w, \quad w(0) = 1. \tag{24}$$

First, we want to drive $w(z,t)$ to $w(t_f) = 1/2$. Setting $\phi = 1$, the characteristic curves of (24) solve $\dot{z} = \mu z$, and are given by $z(t) = z_0\exp(\mu t)$. Along the characteristic curves, $w(z(t),t)$ satisfies the ordinary differential equation

$$\frac{\partial w}{\partial t} = -\mu w - k\gamma c w, \quad w(0) = 1.$$

This equation can be solved explicitly, but the quantity of interest for optimal control is the linear Bucy-Kalman filter. If we set the control term $Bu = -k\gamma c w$, the associated Ricatti equation is

$$\dot{q} = -\mu q + \frac{B^2}{R}q^2 - S, \quad q(t_f) = 1,$$

with solution

$$q(t) = \frac{\alpha}{\beta(1-\exp(\alpha t))} - \frac{\alpha}{\beta(1-\exp(\alpha t_f))} + 1,$$

where $\alpha = 2(-\mu + \frac{B^2}{R})$ and $\beta = \frac{B^2}{R}$. Starting at some small $t > 0$, to avoid the singularity $q(0) = \infty$, the Bucy-Kalman filter

$$Bu = -\frac{B^2}{R}qw = -k\gamma c w,$$

with $B = \sqrt{k\gamma R}$, $c = q$, will drive w down to $1/2$, in time t_f.

Next, we wish to drive w from $1/2$ to 0. Now, we linearize about small $\phi = \epsilon$

$$\dot{w} = \mu(1-2\epsilon)w - \frac{kc\gamma}{\epsilon^{1-\gamma}}w = \mu(1-2\epsilon)w + Bu.$$

Starting from $w(0) = 1/2$, we can drive w to zero with the Bucy-Kalman filter defined by the Ricatti equation

$$\dot{q} = -2\mu(1-2\epsilon)q + \frac{B^2}{R}q^2 - S, \quad q(t_f) = 1.$$

The solution of this equation is

$$q = \alpha - \sqrt{\alpha^2+\beta}\left(\frac{a + e^{b(t_f - t)}}{a - e^{b(t_f-t)}}\right)$$

where $\alpha = R\mu(1-2\epsilon)/B^2$, $\beta = \frac{RS}{B^2}$, $a = \frac{1-\alpha-\sqrt{\alpha^2+\beta}}{1-\alpha+\sqrt{\alpha^2+\beta}}$ and $b = \frac{2R}{B^2}\sqrt{\alpha^2+\beta}$. This filter will drive w to zero at t_f, considering a control term

$$Bu = -\frac{B^2}{R}qw = -\frac{kc\gamma}{\epsilon^{1-\gamma}}w,$$

which can be large because $1-\gamma > 0$ and ϵ is small.

6.3. Optimal control of biofilms

We start with the equation

$$\frac{\partial \phi}{\partial t} + v\frac{\partial \phi}{\partial z} = \mu(e)(\phi - \phi^2) - k_{a_1}(e)C_{a_1}\phi^{\gamma_1} - k_{a_2}(e)C_{a_2}\phi^{\gamma_2},$$

where $v(z,t) = \int_0^z \mu\phi ds$. We let $\phi = \phi_0 + \phi_1$, where ϕ_0 is a solution of the above (uncontrolled) equation

$$\frac{\partial \phi_0}{\partial t} + v\frac{\partial \phi_0}{\partial z} = \mu(e)(\phi_0 - \phi_0^2).$$

Linearizing about ϕ_0, and with the controls added, we find

$$\frac{\partial \phi_1}{\partial t} + v_0\frac{\partial \phi_1}{\partial z} + v_1\frac{\partial \phi_0}{\partial z} = \mu(e)(1-2\phi_0)\phi_1 - \gamma_1 k_{a_1}(e)C_{a_1}\frac{1}{\phi_0^{1-\gamma_1}}\phi_1 - \gamma_2 k_{a_2}(e)C_{a_2}\frac{1}{\phi_0^{1-\gamma_2}}\phi_1, \tag{25}$$

where $v_0(z,t) = \int_0^z \mu\phi_0 ds$ and $v_1(z,t) = \int_0^z \mu\phi_1 ds$. Then we find a linearized regulator where the cost function is

$$J(\phi_1) = \frac{1}{2}\langle\phi_1(T), P\phi_1(T)\rangle + \frac{1}{2}\int_0^T \langle\phi_1(t), S\phi_1(t)\rangle + \langle U(t), RU(t)\rangle dt,$$

with T the terminal time.

Now Eq. (25) can be written in the form

$$\frac{\partial\phi_1}{\partial t} = A\phi_1 + BU,$$

$U^t = (u_1, u_2)$, where A is the linear operator

$$A = -v_0\frac{\partial}{\partial z} - \frac{\partial\phi_0}{\partial z}\int_0^z \mu(\cdot)ds + \mu(1-2\phi_0),$$

and $B = -(C_{a_1}\gamma_1 k_{a_1}\phi_0^{\gamma_1-1}, C_{a_2}\gamma_2 k_{a_2}\phi_0^{\gamma_2-1})$. The Kalman gain is

$$K(t) = R^{-1}B^*Q(t),$$

where

$$\dot{Q}(t) = -Q(t)A - A^*Q(t) + Q(t)BR^{-1}B^*Q(t) - S, \qquad Q(T) = P, \tag{26}$$

and $\lambda(T) = P\phi_1(T) = -P\phi_0(T)$. Notice that the final value of the Lagrange multiplier λ imples that the final value of $\phi(T) = \phi_0(T) + \phi_1(T) = 0$. Eq. (26) is solved backwards with the terminal condition $Q(T)$. The controls become

$$U(t) = -R^{-1}B^*\lambda(t) = K(t)\phi_1(t).$$

If we choose $R = 1/r$, $S = s$ and $P = 1$ to be constants, we get the Ricatti equation

$$\dot{Q}(t) = -Q(t)A - A^*Q(t) + rQ(t)(C_{a_1}^2\gamma_1^2k_{a_1}^2\phi_0^{2(\gamma_1-1)} + C_{a_2}^2\gamma_2^2k_{a_2}^2\phi_0^{2(\gamma_1-1)})Q(t) - s,$$

with $Q(T) = 1$, and the control

$$BU(t) = r(C_{a_1}\gamma_1 k_{a_1}\phi_0^{(\gamma_1-1)} + C_{a_2}\gamma_2 k_{a_2}\phi_0^{(\gamma_2-1)})Q(t)\phi_1(t).$$

We can choose r and s to be any positive constants.

The optimal control is implemented in the two steps described in the previous section. In practice, in our tests the second step starting from 1 has been enough to drive the system to zero, see Fig. 6(b)–(c).

7. Numerical schemes

Model (4)–(10) contains a transport problem set in a moving domain together with diffusion submodels evolving in different time scales, which must be properly addressed to achieve reliable schemes. We sketch here the numerical schemes employed. Consider a grid (z^n, t^m), $z^n = n\delta z$, $t^m = m\delta t$, $n = 0, \dots, N$, $m = 0, \dots, M$, with $\delta z = \frac{L}{M}$ and $\delta t = \frac{T}{M}$. We discretize the equations in such a way that the stability bounds $0 \le \phi_1 \le 1$, $0 \le C_0 \le c_o$, $0 \le C_{a_1} \le c_{a_1}$ and $0 \le C_{a_2} \le c_{a_2}$ are satisfied and the constraint $0 \le \phi \le 1$ is satisfied.

7.1. The transport submodel

We consider simulations of a shrinking biofilm for which the moving boundary retracts, that is, $L(t)$ decreases with time. We discretize Eq. (4) by means of an upwind scheme and Eqs. (6)–(7) by means of forward differences:

$$\begin{aligned}
&\frac{\phi_{n,m+1}-\phi_{n,m}}{\delta t} + \frac{v_{n,m}\phi_{n,m} - v_{n-1,m}\phi_{n-1,m}}{\delta z} = -k_{a_1}(e_{n,m})(C_{a_1})_{n,m}\phi_{n,m}^{\gamma_1}\\
&-k_{a_2}(e_{n,m})(C_{a_2})_{n,m}\phi_{n,m}^{\gamma_2} + \mu(e_{n,m})\phi_{n,m}, \quad 0 < n \le b_m = [L_m/\delta z], 0 \le m,\\
&\phi_{n,0} = 1, \quad 0 < n \le b_0 = [L_0/\delta z], 0 \le m,\\
&\frac{v_{n,m}-v_{n-1,m}}{\delta z} = \mu(e_{n,m})\phi_{n,m}, \quad 0 < n < b_m, 0 \le m,\\
&v_{0,m} = 0, \quad 0 \le m,\\
&\frac{L_{m+1}-L_m}{\delta t} = v(L_m, t_m) - k_d L_m^2, \quad 0 \le m.
\end{aligned} \tag{27}$$

The truncation error is $O(\delta t + \delta z)$. This scheme relies on the positivity of $\phi_{n,m}$ to guarantee the positivity of the velocity $v_{n,m}$ and the stability of the selected upwind discretization under a CFL condition $\delta t < \frac{1}{\max(v)}\delta z$. Under the constraint $0 \le \phi_{n,m} \le 1$, we have $0 \le v_{n,m} \le \mu_{\max}L(0)$. Notice that we do not need a boundary condition at $n = 0$ for ϕ since $v(0,t) = 0$. Moreover, we do not need a boundary condition at $L(t)$ as long as the characteristic curves enter that boundary [24]. As we explain in Section 7.2, $(C_o)_{n,m}$, $(C_{a_1})_{n,m}$, $(C_{a_2})_{n,m}$, are calculated by a quasi-stationary approximation. They are positive and bounded from above by the boundary values. As a result, $0 \le e_{n,m} \le e_{\max} \le 1$.

Let us see how the positivity constraints for ϕ and $1-\phi$ are preserved from one step to the next choosing δt small enough. We have the scheme

$$\phi_{n,m+1} = \phi_{n,m} - \frac{\delta t}{\delta z}(v_{n,m}\phi_{n,m} - v_{n-1,m}\phi_{n-1,m}) + \delta t(\mu(e_{n,m})\phi_{n,m} - k_{a_1}(e_{n,m})(C_{a_1})_{n,m}\phi_{n,m}^{\gamma_1} - k_{a_2}(e_{n,m})(C_{a_2})_{n,m}\phi_{n,m}^{\gamma_2})$$

for $0 \le n \le b_m \le N$. Initially, $0 \le \phi_{n,0} \le 1$ for all $0 \le n \le b_0$. By induction on m, we assume $0 \le \phi_{n,m} \le 1$ for all $0 \le n \le b_m$, and check the constraint for $m+1$. We have $v_{n,m} \le \mu_{\max} L$. Moreover, the last terms in the scheme are smaller than $(\mu(e) - k_{a_1}(e)C_{a_1} - k_{a_2}(e)C_{a_2})_{n,m}\phi_{n,m}^{\gamma}$, $\gamma = \min(\gamma_1, \gamma_2)$. We assume $\delta t/\delta z < 1/(\mu_{\max} L)$ and $(\mu(e) - k_{a_1}(e)C_{a_1} - k_{a_2}(e)C_{a_2})_{n,m} \le 0$. Then

$$\begin{aligned}\phi_{n,m+1} &\le \Big(1 - \frac{\delta t}{\delta z}v_{n,m}\Big)\phi_{n,m} + \frac{\delta t}{\delta z}v_{n-1,m}\phi_{n-1,m}\\ &\le \Big(1 - \frac{\delta t}{\delta z}v_{n,m} + \frac{\delta t}{\delta z}v_{n-1,m}\Big)\max_n\phi_{n,m} \le \max_n\phi_{n,m} \le 1\end{aligned}$$

Notice that $v_{n,m} - v_{n-1,m} \ge 0$, for all n, since we are assuming $\phi_{n,m} \ge 0$. On the other hand, given $\phi_{n,0} = 1$, $n = 0, \dots, N$,

$$\phi_{n,1} = \Big(1 - \frac{\delta t}{\delta z}(v_{n,m} - v_{n-1,m})\Big) + \delta t(\mu(e) - k_{a_1}(e)C_{a_1} - k_{a_2}(e)C_{a_2})_{n,m}.$$

For δt small, $\phi_{n,1} > 0$ $n = 0, \dots, N$. This situation will continue until a value of m at which this condition fails. In our simulations, the solution vanishes in finite time. Due to the choice of parameters, the physical boundary retracts according to

$$L_{m+1} = L_m + \big(v(L_m, t_m) - k_d L_m^2\big)\delta t.$$

We locate the new boundary at b_{m+1}, the integer part of $L_{m+1}/\delta z$.

7.2. The diffusion submodels

The diffusion submodels are solved in a fixed domain $[0, L_{\max}] \times [0, T]$ with a transmission boundary condition at the moving interface $L(t)$, $t > 0$. Source terms are only active inside the film.

For the parameter values employed in our simulations, the transport problem evolves in a time scale t of hours, while chemicals diffuse in a time scale s of seconds. At each time step t_m of the transport scheme, knowing the approximate values of $\phi_l(t_m)$, we use quasi-stationary fields $(C_o)_{n,m}$, $(C_a)_{n,m}$, $(C_o)_{n,m}$ that approximate the solutions of

$$\begin{aligned}&0 = \frac{\partial}{\partial z}\left(d_o\frac{\partial C_o}{\partial z}\right) - k_o\frac{C_o}{C_o + K_o}\phi_l(t_m)\chi_{[0,L(t_m)]}\phi_c\rho_x, \qquad 0 \le z \le L_{\max},\\ &\frac{\partial C_o}{\partial z}(0) = 0,\ C_o(L_{\max}) = c_o,\end{aligned} \tag{28}$$

$$\begin{aligned}&0 = \frac{\partial}{\partial z}\left(d_a\frac{\partial C_a}{\partial z}\right) - k_a C_a\phi_l(t_m)\chi_{[0,L(t_m)]}\phi_c\rho_x, \qquad 0 \le z \le L_{\max},\\ &\frac{\partial C_a}{\partial z}(0) = 0,\ C_a(L_{\max}) = c_a,\end{aligned} \tag{29}$$

for $a = a_1, a_2$. We can solve these problems by finite elements [27]. For each of them, we write $C_i = c_i + \tilde{C}_i$, $i = o, a_1, a_2$, and consider $H = H^1(0, L_{\max}) \cap \{\tilde{C}(L_{\max}) = 0\}$. For each $N > 0$, let $\{\psi_1, \dots, \psi_N\}$ a finite element basis of H. Then, we mimic in V^N the steps described in the proof of Theorem 1 in Section 8 to prove existence of a unique solution $C_i = c_i + \tilde{C}_i$, $\tilde{C}_i \in H$ of (29), $a = a_1, a_2$ and (28) in H. In this way, we obtain approximate solutions $C_{a_1}^N$ and $C_{a_2}^N$ whose coefficients are determined solving linear matricial systems and approximate solutions C_o^N whose coefficients are found through an iterative scheme to solve a nonlinear matricial system. These solutions enjoy the same sign properties as stated in Theorem 1: $0 \le C_{a_1}^N \le c_{a_1}$, $0 \le C_{a_2}^N \le c_{a_2}$ and $0 \le C_o^N \le c_o$.

In the next section, we establish the well posedness results on the model which ensure the reliability of these numerical schemes.

8. Well posedness results for the model

Trustworthiness of simulations and estimates relies on the well posedness properties of the original model. Notice that the transport problem is set in a domain with a moving boundary, while standard theories focus on problems set in domains with fixed boundaries. Next, we establish well posedness results for our model and show that essential positivity constraints are satisfied.

8.1. The reaction-diffusion submodels

As explained in Section 7.2, for the parameter values employed in our simulations, the transport problem evolves in a time scale t of hours, while chemicals diffuse in a time scale s of seconds. This leads to a quasi-stationary approximation in which at each time in the transport scale, the reaction-diffusion models for oxygen and antibiotic concentrations are stationary and are approximated by elliptic problems whose sources and boundary points depend on time.

Given $L(t) \in C([0,T])$, we set $\Omega_T = \cup_{t\in[0,T]}[0,L(t)]\times\{t\}$. For $\phi_l \in L^\infty(\Omega_T)$, with $0 \le \phi_l \le 1$, we consider the elliptic problems

$$\begin{aligned} 0 &= \frac{\partial}{\partial z}\left(d_o \frac{\partial C_o}{\partial z}\right) - \frac{k_o \phi_c \rho_x}{C_o + K_o}\phi_l \chi_{[0,L(t)]} C_o, \quad 0 \le z \le L_{\max}, t > 0, \\ &\frac{\partial C_o}{\partial z}(0) = 0, \quad C_o(L_{\max}) = c_o, \end{aligned} \tag{30}$$

$$\begin{aligned} 0 &= \frac{\partial}{\partial z}\left(d_a \frac{\partial C_a}{\partial z}\right) - k_a \phi_c \rho_x \phi_l \chi_{[0,L(t)]} C_a, \quad 0 \le z \le L_{\max}, t > 0, \\ &\frac{\partial C_a}{\partial z}(0) = 0, \quad C_a(L_{\max}) = c_a, \end{aligned} \tag{31}$$

for a = a$_1$,a$_2$, with $c_o, c_a > 0$. We have the following result.

Theorem 1. *Assume that $\phi_l, d_o, d_a \in L^\infty(0, L_{\max})$ for each fixed t, $0 \le \phi_l \le 1$, and d_o, d_a, c_o, c_a are positive. For each $t \in [0,T]$, systems (30) and (31) admit unique solutions $C_o \in H^1(0, L_{\max})$ and $C_a \in H^1(0, L_{\max})$, $a = a_1, a_2$ for each $t \in [0,T]$. These solutions satisfy*

- $0 \le C_o \le c_o$, $0 \le C_a \le c_a$,
- $C_o \in H^2(0, L(t)) \cap C^1([0, L(t)])$, $C_a \in H^2(0, L(t)) \cap C^1([0, L(t)])$,
- C_o *and* C_a *are nondecreasing functions of* z.

Moreover, if $\phi_l \in C([0,T])$, then C_o and C_a are continuous functions of t in Ω_T.

Proof. Let us fix a time $t \in [0,T]$. Systems (30) and (31) are elliptic problems with coefficients in $L^\infty(0, L_{\max})$. Let us define the Hilbert space $H = \{\tilde{C} \in H^1(0, L_{\max}) | \tilde{C}(L_{\max}) = 0\}$, where $H^1(0, L_{\max})$ is the standard Sobolev space [6,27]. We set $C_o = c_o + \tilde{C}_o$, $C_a = c_a + \tilde{C}_a$, with $\tilde{C}_o, \tilde{C}_a \in H$. In variational form, the linear problem (31) reads: Find $\tilde{C}_a \in H$ such that

$$\int_0^{L_{\max}} \left[d_a \frac{\partial \tilde{C}_a}{\partial z}\frac{\partial w}{\partial z} + k_a \phi_c \rho_x \phi_l \chi_{[0,L(t)]} \tilde{C}_a w\right] dz = -\int_0^{L_{\max}} k_a \phi_c \rho_x \phi_l \chi_{[0,L(t)]} c_a w \, dz \tag{32}$$

for $w \in H$. The left hand side defines a continuous bilinear form $b(c,w)$ in $H \times H$, which is symmetric and coercive. The right hand side defines a continuous linear form $\ell(w)$ in H. By Lax Milgram's theorem, there is a unique solution $\tilde{C}_a \in H$ [6,27]. By Sobolev injections, $\tilde{C}_a \in C([0,L])$ [6]. Using the positive part as a test function $w = \tilde{C}_a^+$ [6], we get $\tilde{C}_a^+ = 0$ and $\tilde{C}_a \le 0$. On the other hand,

$$\int_0^{L_{\max}} \left[d_a \frac{\partial C_a}{\partial z}\frac{\partial w}{\partial z} + k_a \phi_c \rho_x \phi_l(t) \chi_{[0,L(t)]} C_a w\right] dz = 0.$$

Taking $w = C_a^-$, we obtain $C_a^- = 0$. Therefore, $0 \le C_a \le c_a$. By elliptic regularity, the solution we seek, $C_a = c_a + \tilde{C}_a$, belongs to $H^2(0, L_{\max})$ and $C^1([0, L_{\max}])$, at least [6]. Morover, using $w = \tilde{C}_a$ as a test function in (32), we find $\|\nabla C_a\|_{L^2(0,L_{\max})} \le k_a c_a \phi_c \rho_x L_{\max}^{\frac{1}{2}}/(\min(d_a) S_{\max})$, $S_{\max}$ being Sobolev's constant [27]. Integrating (31) we obtain

$$d_a \frac{\partial C_a(z)}{\partial z} = k_a \phi_c \rho_x \int_0^z \phi_l(s,t) C_a(s)\, ds \ge 0,$$

so that C_a is nondecreasing.

The nonlinear problem (30) requires an iterative procedure. Consider the problem: Find $\tilde{C}_o^\ell \in H$ such that

$$\int_0^{L_{\max}} \left[d_o \frac{\partial \tilde{C}_o^\ell}{\partial z}\frac{\partial w}{\partial z} + \frac{k_o \phi_c \rho_x}{C_o^{\ell-1} + K_o}\phi_l \chi_{[0,L(t)]} \tilde{C}_o^\ell w\right] dz = -\int_0^{L_{\max}} \frac{k_o \phi_c \rho_x}{C_o^{\ell-1} + K_o}\phi_l \chi_{[0,L(t)]} c_o w \, dz \tag{33}$$

for $w \in H$, starting from $\tilde{C}_o^0 = 0$. Given $C_o^{\ell-1}$ such that $0 \le C_o^{\ell-1} \le c_o$, this is an elliptic linear problem similar to the one satisfied by C_a, with bounded coefficients. Existence of a solution $\tilde{C}_o^\ell \in H$ follows from Lax Milgram's theorem. By similar maximum principles and regularity theory, we obtain $0 \le C_o^\ell = \tilde{C}_o^\ell + c_o \le c_o$ and $C_o^\ell \in C([0, L_{\max}])$. These estimates remain true for all ℓ by induction. Moreover, using $w = \tilde{C}_o^\ell$ as a test function in (33), we find

$$\int_0^{L_{\max}} \left[d_o \left|\frac{\partial \tilde{C}_o^\ell}{\partial z}\right|^2 + \frac{k_o \phi_c \rho_x}{C_o^{\ell-1} + K_o}\phi_l \chi_{[0,L(t)]} |\tilde{C}_o^\ell|^2\right] dz = -\int_0^{L_{\max}} \frac{k_o \phi_c \rho_x}{C_o^{\ell-1} + K_o}\phi_l \chi_{[0,L(t)]} c_o \tilde{C}_o^\ell \, dz \le \frac{k_o c_o \phi_c \rho_x}{K_o} L_{\max}^{\frac{1}{2}} \|\tilde{C}_o^\ell\|_{L^2(0,L)}.$$

Poincare's inequality in H implies that $\|\nabla C_o^\ell\|_{L^2(0,L_{\max})} \le \frac{k_o c_o \phi_c \rho_x L^{\frac{1}{2}}}{\min(d_o) K_o S_{\max}} = M$, $S_{\max}$ being Sobolev's constant [27]. Since C_o^ℓ is uniformly bounded in $H^1(0, L_{\max})$ for $\ell \ge 0$ and the injection in $L^2(0, L_{\max})$ is compact, a subsequence $C_o^{\ell'}$ tends weakly to a limit $C_o = \tilde{C}_o + c_o$ in $H^1(0, L_{\max})$, strongly in $L^2(0, L_{\max})$ and pointwise, a.e. in $(0, L_{\max})$. Passing to the limit as $\ell' \to \infty$ in (33), we find that $C_o = c_o + \tilde{C}_o$ is the solution of (30). This solution is continuous and inherits the estimate $0 \le C_o \le c_o$. By elliptic regularity, it belongs to $H^2(0, L(t))$ and $C^1([0, L(t)])$, at least. As before, we prove that C_o is nondecreasing.

Uniqueness follows by contradiction. We assume there are two positive solutions C_1 and C_2 and set $C = C_1 - C_2 \in H$. Subtracting the equations we see that C is a solution to

$$\int_0^{L_{\max}} \left[d_o \frac{\partial C}{\partial z}\frac{\partial w}{\partial z} + \frac{k_o \phi_c \rho_x}{(C_1 + K_o)(C_2 + K_o)}\phi_l \chi_{[0,L(t)]} C w\right] dz = 0 \tag{34}$$

for all $w \in H$. Taking $w = C$, we conclude that $C = 0$, that is, $C_1 = C_2$.

Continuity with respect to t inside Ω_T follows comparing the solutions for $t' \to t$ in balls contained in Ω_T. □

This theorem defines families of solutions C_{a_1}, C_{a_2} and C_o of (31) and (30) for $t \in [0, T]$. In this paper, the values we employ for the diffusivities lead to a quasi-static approximation in the simulations. The full parabolic sub-models (9) and (10) should be simulated for other choices, given functions $\phi_l \in L^\infty((0, L) \times (0, T))$, with $0 \le \phi_l \le 1$.

8.2. The transport submodel

Given nonnegative and continuous functions C_o, C_{a_1} and C_{a_2} which satisfy the properties stated in Theorem 1, we study now the transport problem (4). Constructing weak solutions to the transport problem under general hypotheses is quite technical, see [32], for instance. Here, we establish some basic results by the method of characteristics in a particular situation.

Theorem 2. *Let C_{a_1}, C_{a_2}, C_o be continuous functions in $\cup_{t\in[0,T]}[0, L(t)] \times \{t\} = \Omega_T$ satisfying $0 \le C_i \le c_i$, $i = a_1, a_2, o$, which are nondecreasing with respect to z. Then, the transport problem (4) admits solutions constructed by the method of characteristics satisfying $0 \le \phi_l \le 1$ up to a time τ. If $\mathcal{T} = \{t \le T \,\big|\, \exists \xi \in (0, L(t))\ s.t.\ \phi_l(\xi, t) = 0 \text{ and } \exists \delta \in (0, \xi)\ s.t.\ \phi_l(\xi - \delta, t) \ne 0\} = \emptyset$, $\tau = T$, otherwise τ is at least $\min\mathcal{T}$.*

Proof. We consider the equation

$$\frac{\partial \phi_l}{\partial t} + v\frac{\partial \phi_l}{\partial z} = \mu(e)(\phi_l - \phi_l^2) - k_{a_1}(e)C_{a_1}\phi_l^{\gamma_1} - k_{a_2}(e)C_{a_2}\phi_l^{\gamma_2}, \quad 0 < z < L(t), \tag{35}$$

where $v = \int_0^z \mu(e)\phi_l(x,t)dx$, $e = \frac{C_o}{C_o + K_o}$, $\mu(e)$, $k_{a_1}(e)$ and $k_2(e)$ defined in (8) with $\mu_{\max}$, K_o, k_{a_1}, $k_{a_2} > 0$, and $\phi_l(z, 0) = 1$ in $[0, L(0)]$. Notice that $0 \le \mu(e) \le \mu_{\max}$, $0 \le k_{a_1}(e) \le k_1 e_{\max}$ and $0 \le k_{a_2}(e) \le k_2 e_{\max}$. We set $f(z, \phi_l, t) = -k_{a_1}(e)C_{a_1}\phi_l^{\gamma_1} - k_{a_2}(e)C_{a_2}\phi_l^{\gamma_2}$. The characteristic curves for (35) are the solutions of

$$z'(t; z_0) = \int_0^{z(t;z_0)} \mu(e(x,t))\phi_l(x,t)\,dx,\ t \ge 0, \quad z(0; z_0) = z_0. \tag{36}$$

Since $0 \le \mu(e) \le \mu_{\max}$, the right hand side is a Lipschitz function of $z(t)$ as long as we keep $0 \le \phi_l \le 1$. Unique global solutions can be constructed under such conditions.

Along the characteristic curves $z(t; z_0)$, a solution ϕ_l of (35) satisfies

$$\begin{aligned} &\frac{\partial \phi_l(z(t), t))}{\partial t} = \mu(e(z(t), t))(\phi_l(z(t), t) - \phi_l(z(t), t)^2) + f(z(t), \phi_l(z(t), t), t), \\ &\phi_l(z_0, 0) = 1. \end{aligned} \tag{37}$$

Setting $\phi(t) = \phi_l(z(t), t)$, we have a system of coupled ordinary differential equations for the unknown functions $z(t)$ and $\phi(t)$, which exist globally in t provided we exclude blow-up in finite time.

In view of the initial condition, $\phi_l(z(t), t))$ remains positive for a time $[0, \tau]$, $\tau > 0$. Eq. (37) implies that $\phi_l(z(t), t))$ cannot grow beyond 1 because the derivative is negative when $\phi_l = 1$. In case $\phi_l(z(\tau), \tau) = 0$, the powers γ_1 and γ_2 in $(0, 1)$ force $\phi_l(z(t), t) = 0$ for $t \ge \tau$. Therefore, $\phi_l(z(t), t))$ remains positive and smaller than one. Blow up in finite time is excluded.

The solution to (35) can be constructed everywhere using the characteristic curves provided that

i) for each point (z, t) in the computational domain we can find $z_0 \in [0, L(0)]$ such that the corresponding characteristic curve reaches z at time t, that is, $z(t; z_0) = z$,
ii) no point z is reached by two different characteristic curves, that is, we cannot find (z_1, t_1) and (z_2, t_2) such that $z(t_1; z_1) = z = z(t_2; z_2)$.

Assume that $z_{0,1} < z_{0,2}$. Differentiating the integral formulation of (36) with respect to z_0 we find

$$z_{z_0}(t; z_0) = 1 + \int_0^t \mu(e(z(s; z_0), s))\phi_l(z(s; z_0), s)z_{z_0}(s; z_0)ds.$$

Then, $z_{z_0}(t; z_0)$ is a solution of the differential equation

$$z'_{z_0}(t; z_0) = \mu(e(z(t; z_0), s))\phi_l(z(t; z_0), s)z_{z_0}(t; z_0),\ t \ge 0, \quad z_{z_0}(0; z_0) = 1, \tag{38}$$

which implies $z_{z_0}(t; z_0) \ge 0$, $t \ge 0$. Therefore, if $z_{0,1} < z_{0,2}$, then $z(t; z_{0,1}) \le z(t; z_{0,2})$, for $t > 0$. As long as $z_{z_0}(t; z_0) > 0$, we can invert and find $z_0(z, t)$ for each couple (z, t) and i) and ii) are guaranteed. This holds as long as ϕ_l does not vanish.

Exceptions may arise when ϕ_l vanishes. If $\phi_l(z(\tau; z_1), \tau) = 0$, the slope of the characteristic curve $t(z; z_1)$ in the (z, t) plane is vertical and $\phi_l(z(t; z_1), t) = 0$ along that vertical curve. We can exclude that $z(t; z_1)$ meets $z(t; z_2)$ at any τ. If $\phi_l(z(\tau; z_2), \tau) = 0$, the slope of the characteristic curve $t(z; z_2)$ in the (z, t) plane is vertical and $\phi_l(z(t; z_2), t) = 0$. We cannot exclude that $z(t; z_1)$ meets $z(t; z_2)$ at a time τ without further hypotheses. □

Remark. Notice that the numerical scheme described in Section 7 does not rely on characteristics and works for general solutions of conservation laws, even when they present shocks or rarefactions.

In our simulations ϕ_l starts vanishing from 0 outwards due to the antibiotic targeting dormant cells and from $L(t)$ inwards due to the antibiotic targeting active cells. The first situation results in characteristics becoming vertical and ϕ_l vanishing sequentially along them as z_0 grows from zero. The second situation results in the boundary $L(t)$ retracting as ϕ_l vanishes at boundary points. This dynamics avoids shocks and would allow us to construct solutions by the characteristic method as in Theorem 2.

Remark. If we set $\gamma_1, \gamma_2 \ge 1$, ϕ_l does not vanish in finite time, and $\tau = T$. Theorem 2 might hold without that time constraint.

8.3. Coupling the submodels

In this section we combine the results stated in the previous two sections to obtain an existence result for the whole system.

Theorem 3. *Given positive parameters* $L_{\max}$, $\mu_{\max}$, k_1, k_2, k_d, c_{a_1}, k_{a_1}, c_{a_2}, k_{a_2}, c_o, k_o, K_o, ρ_x, $0 < \gamma_1, \gamma_2 < 1$, *and nonnegative functions* ϕ_c, d_{a_1}, d_{a_2}, $d_o \in L^\infty(0, L_{\max})$, $L_{\max} > \frac{\mu_{\max}}{k_d}$, *the transport problem (4)–(6) coupled to equations (28)–(29) with* $L(t)$ *given by (7),* $L(0) \in (0, L_{\max})$, *and* $\mu(e)$, $k_{a_1}(e)$, $k_{a_2}(e)$ *given by (8) admits a solution* $L \in C^1([0,\tau])$, $\phi_l \in C^1(\Omega_\tau)$, $C_o, C_{a_1}, C_{a_2} \in C(\Omega_\tau)$, *satisfying* $0 \le \phi_l \le 1$, $0 \le C_i \le c_i$, $i = o, a_1, a_2$ *and the additional estimates established in Theorems 1 and 2 at least up to the first inner vanishing time* $\tau \le T$.

Proof. We initialize an iterative scheme as follows. Set $L^0(t) = L(0)$, $t \ge 0$, and $\phi_l^0 = 1$, and solve (30)–(31) to get $C_o^0, C_{a_1}^0, C_{a_2}^0$ satisfying the properties stated in Theorem 1. Next, we apply Theorem 2 to construct a solution ϕ_l^1 of (4)–(6) and calculate $L^1(t)$ solving (7). We iterate this process to construct a sequence of functions

- L^ℓ that solve (7) for ϕ_l^ℓ and $C_o^{\ell-1}$,
- $C_o^\ell, C_{a_1}^\ell, C_{a_2}^\ell$ that solve (30)–(31) for L^ℓ and ϕ_l^ℓ,
- $\phi_l^{\ell+1}$ that solve (4)–(6) for L^ℓ and $C_o^\ell, C_{a_1}^\ell, C_{a_2}^\ell$

satisfying the properties stated in Theorems 1 and 2 up to a time $\tau^{\ell+1} \le \tau^\ell$. Let $\tau = \inf_\ell \tau^\ell$.

Identity (7) for L^ℓ implies that the sequence is equicontinuous. Since $L(0) \in (0, L_{\max})$, L^ℓ will remain positive at least up to a time τ^ℓ, while the right hand side of (7) is bounded from above by $(\mu_{\max} - k_d L^\ell(t))L^\ell(t)$. This term is negative if $L^\ell(t) > \frac{\mu_{\max}}{k_d}$, thus $L^\ell(t) \le L_{\max}$ for $t \in [0,T]$. Now, $-k_d L_{\max}^2 \le -k_d (L^\ell)^2 \le L_t^\ell \le \mu_{\max} L_{\max}$. By Ascoli-Arzelá's Theorem, we can extract a subsequence L^{ℓ_k} that converges uniformly to a continuous limit $L < L_{\max}$ in $C([0,\tau])$.

By Theorem 1, we know that the functions $C_o^\ell, C_{a_1}^\ell, C_{a_2}^\ell$ are uniformly bounded in $L^\infty([0, L_{\max}] \times [0, \tau^\ell])$ and $C_{o,z}^\ell, C_{a_1,z}^\ell, C_{a_2,z}^\ell$ are uniformly bounded in terms of the parameters of the problem provided $0 \le \phi_l^\ell \le 1$, that is ensured by Theorem 2. For each fixed $t \le \tau$, these functions converge weakly in $H^1(0, L_{\max})$ and strongly in $L^2(0, L_{\max})$ to limits $C_o(t), C_{a_1}(t), C_{a_2}(t)$. Moreover, due to Sobolev's injections in dimension one, convergence holds in $C([0, L_{\max}])$.

The characteristic curves z^ℓ given by (36) for ϕ_l^ℓ and C_o^ℓ are equicontinuous in $[0,\tau]$. Indeed, $0 \le z_t^\ell \le \mu_{\max} z^\ell$ implies $z_0 \le z^\ell \le z_0 e^{\mu_{\max} t}$, $t \in [0,\tau]$ and a bound on $|z_t^\ell|$ depending on τ. By Ascoli-Arzelá's Theorem, we can extract a subsequence z^{ℓ_k} that converges uniformly to a continuous limit z in $C([0,\tau])$.

The uniform bound $0 \le \phi_l^\ell \le 1$ implies that we can extract a subsequence ϕ^{ℓ_k} converging weakly to a limit ϕ in $L^\infty(\Omega_\tau)$. In view of the strong convergence of $C_o^{\ell_k}$, and z^{ℓ_k}, we can pass to the limit in the integral versions of (36) and conclude that z solves (36) for C_o and ϕ_l. Similarly, we can pass to the limit in the integral versions of (7) and prove that L solves (7) for C_o and ϕ_l. Moreover, taking limits in the variational formulations of (30) and (31), we conclude that C_o, C_{a_1}, C_{a_2} solve (30) and (31) for ϕ_l and L.

Eq. (37) for $\psi^{\ell_k}(t) = \phi_l^{\ell_k}(z^{\ell_k}(t), t)$ implies equicontinuity in $C([0,\tau])$. Again, we can extract a subsequence renamed ψ^{ℓ_k} converging to a limit ψ in $C([0,\tau])$. Passing to the limit in the integral version of the equation, in view of the strong convergences, we conclude that ψ solves (37) for C_o. We can construct the solution of (35) for C_o, C_{a_1}, C_{a_2} and $L(t)$ by the method of characteristics. Now, this solution must be related to the weak limit ϕ_l obtained and used in their construction. For that, just notice that

$$\phi_l^{\ell_k}(z^{\ell_k}(t), t) - \phi_l(z(t), t) = \phi_l^{\ell_k}(z^{\ell_k}(t), t) - \phi_l^{\ell_k}(z(t), t) + \phi_l^{\ell_k}(z(t), t) - \phi_l(z(t), t)$$

The first term tends uniformly to zero due to equicontinuity as ℓ_k tends to infinity. The second term tends to zero a.e. in L^∞ weak.

The limiting functions inherit the bounds established in Theorems 1 and 2 passing to the limit, which provides stability bounds.

9. Conclusion

Fighting implant (catheters, prostheses) associated infections requires the introduction of adequate antibiotic therapies to eradicate biofilms. We consider here a simple model that takes into account basic biofilm features. We show that cocktails of antibiotics adapted to the stratified biofilm structure are able to annihilate in finite time all alive cells for 'slow' death rates, that is, death rates behaving like powers ϕ_l^γ, $0 < \gamma < 1$. When $\gamma = 1$, the volumen fraction of alive cells decreases to zero as time grows. Our estimates of extinction times in terms of model parameters can be used to devise therapies, in particular, regarding antibiotic concentrations, infusion times and frequencies. For practical purposes, we have proposed two antibiotic control implementations to reach biofilm extinction in finite time. First, we develop a bang-bang strategy that relies on the periodic delivery of large antibiotic dosages. Second, we introduce an alternative strategy that infuses lower antibiotic doses. In both cases, the final doses employed to extinguish completely the biofilm are larger that the intermediate doses required to shrink it. This observation could have implications in the reduction of secondary effects when administering antibiotic therapy. To achieve these goals, we have proposed strategies to handle nonlinear control problems in which the underlying uncontrolled systems have two stationary states by combining linearizations about each of them. More sophisticated continuous models [8,18,22] could be analyzed in a similar way.

From the mathematical point of view, studying this kind of models faces relevant technical difficulties, since they are set on domains whose boundary changes with time. We have been able to tackle this difficulty by using a quasi-stationary approximation for the reaction-diffusion concentration equations. Furthermore, well-posedness is established under restrictive conditions on the dynamics of the biofilm boundary, for instance, under the assumption that the biofilm boundary retracts with time to avoid shock development in the transport equation. The analysis of the general problem remains open.

Fractionary power-scaling is known to arise from instance when one drives density equations with white noise. A simple example is provided by the heat equation. Diffusion models for surfaces in grows problems affected by white noise lead to Edward-Wilkinson processes and fractionary growth exponents, $1/2$ in dimension one, see [20]. In our context, how to derive fractionary powers for inserting stochasticity in microscopic model is an open question.

A number of resistance mechanisms are ignored here, such as efflux pumps, increased polymer secretion, acclimation and hypermutability. These mechanisms can be addressed by agent based models coupled to dynamic energy budget rules for bacterial metabolism, which implement stochastic killing laws. While numerical simulations [5,9] show that biofilm extinction can be achieved, analytical studies would require new developments and should be a subject of future work.

CRediT authorship contribution statement

B. Birnir: Writing – review & editing, Methodology, Investigation, Formal analysis, Conceptualization; **A. Carpio:** Writing – review & editing, Writing – original draft, Visualization, Validation, Methodology, Investigation, Funding acquisition, Formal analysis, Conceptualization; **G. Duro:** Writing – review & editing, Methodology, Investigation, Formal analysis.

Data availability

No data was used for the research described in the article.

Declaration of competing interest

The authors declare that they have no known competing financial interests or personal relationships that could have appeared to influence the work reported in this paper.

Acknowledgment

This research has been partially supported by the FEDER/Ministerio de Ciencia, Innovacióny Universidades-Agencia Estatal de Investigación Grants No. PID2020-112796RB-C21 and PID2024-155528OB-C21.

References

[1] Abbas HA, Serry FM, El-Masry EM. Combating *Pseudomonas aeruginosa* biofilms by potential biofilm inhibitors. Asian J Res Pharm Sci 2012;2:66–72.
[2] Anwar H, Costerton JW. Enhanced activity of combination of tobramycin and piperacillin for eradication of sessile biofilm cells of *Pseudomonas aeruginosa*. Antimicrob Agents Chemother 1990;34:1666–71.
[3] Belaud Y. Time-vanishing properties of solutions of some degenerate parabolic equations with strong absorption. Adv Nonlinear Stud 2001;1:117–52.
[4] Besse C, Carles R, Ervedoza S. A conservation law with spatially localized sublinear damping. Annales de l'Institut Henri Poincaré C, Analyse non linéaire 2020;37(1):13–50.
[5] Birnir B, Carpio A, Cebrián E, Vidal P. Dynamic energy budget approach to evaluate antibiotic effects on biofilms. Commun Nonlinear Sci Numer Simul 2018;54:70–83.
[6] Brézis H. Functional analysis, Sobolev spaces and partial differential equations. Springer; 2011.
[7] Carpio A, Duro G. On the solution of boundary value problems set in domains with moving boundaries. Math Methods Appl Sci 2025;48(10):10427–41.
[8] Carpio A, Duro G. Well posedness of fluid-solid mixture models for biofilm spread. Appl Math Model 2023;124:64–85.
[9] Carpio A, González-Albaladejo R. Immersed boundary approach to biofilm spread on surfaces. Commun Comput Phys 2022;31:257–92.
[10] Curtain RF, Zwart H. An introduction to infinite-dimensional linear systems theory. New York: Springer; 1995.
[11] De Beer D, Stoodley P, Roe F, Lewandowski Z. Effects of biofilm structure on oxygen distribution and mass transport. Biotechnol Bioeng 1994;43:1131–8.
[12] Flemming HC, Wingender J. The biofilm matrix. Nat Rev Microbiol 2010;8:623–33.
[13] Høiby N, Bjarnsholt T, Givskov M, Molin S, Ciofu O. Antibiotic resistance of bacterial biofilms. Int J Antimicrob Agents 2010;35: 322–32.
[14] Ince EL. Ordinary differential equations. New York: Dover Publications; 1956.
[15] Jaramayan R. Antibiotic resistance: an overview of mechanisms and a paradigm shift. Curr Sci 2009;96:1475–84.
[16] Kalman RE. Contributions to the theory of optimal control. Bol Soc Mat Mexicana 1960;5:102–19.
[17] Kalman RE. Mathematical description of linear dynamical systems. SIAM J of Contr 1963;1:152–92.
[18] Kapellos GE, Alexiou TS, Payatakes AC. Theoretical modeling of fluid flow in cellular biological media: an overview. Math Biosci 2010;225:83–93.
[19] Kersner R. Nonlinear heat absorption: space localization and extinction in finite time. SIAM J Appl Math 1983;43(6):1274–85.
[20] Kim I, Yang J, Jung Y. A discrete growth model for the Edwards-Wilkinson equation with a conservative noise. J Korean Phys Soc 1999;34(3):314–18.
[21] Lair AV, Oxley ME. Extinction in finite time of solutions to nonlinear absorption-diffusion equations. J Math Anal Appl 1994;182(3):857–66.
[22] Lanir Y. Biorheology and fluid flux in swelling tissues. I. Bicomponent theory for small deformations, including concentration effects. Biorheology 1987;24:173–87.
[23] Lax PD. Hyperbolic systems of conservation laws and the mathematical theory of shock waves. CBMS-NSF Reg Conf Series Appl Math 11. SIAM; 1973.
[24] Leveque RJ. Numerical methods for conservation laws. Birkhauser; 1992.
[25] Lions JL. Optimal control of systems governed by partial differential equations. New York: Springer; 1971.
[26] Misawa M, Nakamura K, Sarkar MAH. A finite time extinction profile and optimal decay for a fast diffusive doubly nonlinear equation. Nonlinear Differ Equ Appl 2023;30:43.
[27] Raviart PA, Thomas JM. Introduction a l'analyse numérique des équations aux dérivées partielles. Masson;1983.
[28] Sage AP, White CC. Optimum systems control. Prentice Hall; 1977.
[29] Sonneborn L, Van Vleck F, The bang-bang principle for linear control systems. SIAM J Contr 1965;2:151–9.
[30] Stewart PS. Mechanisms of antibiotic resistance in bacterial biofilms. Int J Med Microbiol 2002;292:107–13.
[31] Stone PW. Economic burden of healthcare-associated infections: an american perspective. Expert Rev Pharmacoeconomics Outcomes Res 2009;9:417–22.
[32] Tsuge N. Existence of a global solution to a scalar conservation law with a source term for large data. J Math Anal Appl 2015;432:862–7.
[33] Vickery K, Hu H, Jacombs AS, Bradshaw DA, Deva AK. A review of bacterial biofilms and their role in device-associated infection. Healthc Infec 2013;18:61–6.
[34] Werner E, Roe F, Bugnicourt A, Franklin MJ, Heydorn A, Molin S, et al. Stratified growth in *Pseudomonas aeruginosa* biofilms. Appl Environ Microbiol 2004;70:6188–96.